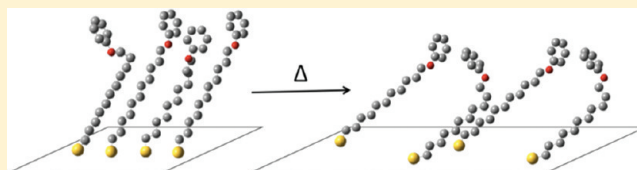


Structural Investigations of the $(5 \times \sqrt{3})$ Striped Phase of Annealed 11-Phenoxy Undecanethiol Self-Assembled Monolayers on Au(111)

Miki Nakayama, Natalie A. Kautz, Tuo Wang, Hanqiu Yuan, and S. J. Sibener*

The James Franck Institute and Department of Chemistry, The University of Chicago, 929 E. 57th Street, Chicago, Illinois 60637, United States

ABSTRACT: Self-assembled monolayers (SAMs) of 11-phenoxyundecanethiol on Au(111) were studied using scanning tunneling microscopy (STM), reflection absorption infrared spectroscopy (RAIRS), ellipsometry, and contact angle measurements before and after annealing in vacuum. The unannealed phenoxy SAM appeared to be disordered under the STM while RAIRS showed that the SAM has relatively significant organization, indicating there is local disordering of the phenoxy groups at the film surface. After annealing, the SAM formed striped domains with a $(5 \times \sqrt{3})$ rectangular structure with respect to the gold substrate. Molecularly resolved STM images of the stripes were obtained, and we were able to see that each stripe consists of two rows of molecules. On the basis of the results from all of the characterization techniques used here, we present a structure for the stripes that involve gauche conformations and the phenyl rings interacting in a favorable edge-to-face configuration. This study shows that mild annealing of aromatic SAMs can lead to drastic structural changes, and that aromatic interactions and electrostatic effects play an important role in determining the final structure.



INTRODUCTION

Self-assembled monolayers (SAMs) are monolayers made of molecules that spontaneously order into a regular pattern without any special external force. The most well-known examples are alkanethiol-based SAMs on Au(111), initially studied by Nuzzo and Allara,¹ and investigated extensively by many researchers using various techniques ever since.^{2–6} Alkanethiol SAMs have attracted a lot of attention because they are robust and easy to prepare. Long-chain alkanethiols with more than nine carbons form high-density SAMs with a $(\sqrt{3} \times \sqrt{3})R30^\circ$ structure with respect to the underlying gold lattice as determined by electron diffraction and scanning tunneling microscopy (STM) studies.^{7,8} According to X-ray diffraction and infrared spectroscopy studies, the chains tilt about 30° from the surface normal to maximize the attractive van der Waals interaction between them.^{9,10}

Alkanethiol SAMs are also of great interest because the molecules can be easily functionalized in virtually any fashion to tune surface properties such as wettability, corrosion inhibition, and electron-transfer properties.^{11–13} Those functionalized with aromatic groups have especially attracted attention due to their delocalized electron distribution which allows for high electrical conductivity, potentially making them useful in molecular electronics.^{14,15} They are also highly anisotropic and have strong intermolecular interactions, making them interesting from a fundamental standpoint on how different molecular interactions affect the structure of the SAM. Much of the earlier studies on aromatic alkanethiol SAMs have been on phenyl-terminated short-chain molecules with only one CH_2 unit between the sulfur and phenyl ring, showing that the molecules form a close-packed structure similar to normal alkanethiols and that the rings pack in a herringbone pattern so that they are

in an edge-to-face configuration.^{16,17} Lee et al. have studied long-chain phenyl-terminated alkanethiol SAMs and also observed that they form well-packed films with the phenyl groups packed in a herringbone structure.¹⁸ Cavadas has conducted a systematic study of long-chain alkanethiol SAMs with a phenyl or phenoxy terminal group, with and without an OH group substitution at the para or meta positions, and found out that the position of the substitution as well as the presence of an ether linkage affect the SAM structure and the orientation of the phenyl rings.¹⁹

Understanding the thermal stability of SAMs is of technological importance for potential applications such as molecular electronics and surface coatings because they typically involve elevated temperatures. The structural effects of annealing SAMs below the desorption temperature have been studied for normal alkanethiol SAMs,^{20,21} but studies on annealing aromatic SAMs are limited. Duan and Garrett have studied the structural changes of 6-phenyl-*n*-hexanethiol SAMs as they were annealed in ultrahigh vacuum (UHV) and observed three different stripe phases.²² They believed the structures were composed of the molecules either lying flat on the substrate or tilted out of the surface plane by gauche defects near the sulfur atom, based on the interstripe spacing and on previous studies of striped phases of normal alkanethiols.²² Lee et al. have studied pyrrolyl-terminated alkanethiol SAMs with 11 or 12 carbons annealed in solution.²³ The unannealed pyrrolyl-terminated SAMs were disordered, but after annealing, a stripe phase with a $(5 \times \sqrt{3})$ rectangular structure was

Received: December 17, 2011

Revised: February 10, 2012

Published: March 1, 2012

observed.²³ Lee et al. proposed that dipole–dipole interactions and gauche defects cause disorder in the unannealed SAM, and that a combination of herringbone-like and parallel-shifted packing of the pyrrolyl groups helps to relieve the destabilizing dipole interactions in the annealed SAMs.²³ Both of the above studies used STM as part of their investigation, but molecular resolution was not obtained.

In this work, we study SAMs of 11-phenoxy undecanethiol on Au(111) before and after annealing in UHV using STM, reflection absorption infrared spectroscopy (RAIRS), ellipsometry, and water contact angle measurements. The structural formula of the molecule along with its dimensions is given in Figure 1. Phenoxy-terminated SAMs are especially interesting

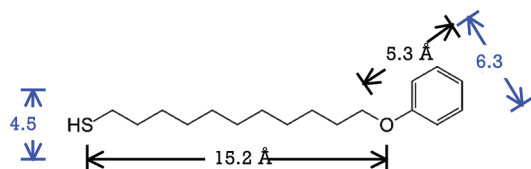


Figure 1. Structural formula of 11-phenoxy undecanethiol with its molecular dimensions (black lines) and van der Waals diameters (blue lines).

because they have been shown to have a high propensity for adsorbing proteins,²⁴ making them potentially useful in biological applications, but few studies have been done on them. We are especially unaware of any STM studies on the structure of phenoxy-terminated SAMs. STM is suitable for structural investigations of SAMs because it provides images of the local topography, and scanning tunneling spectroscopy (STS) provides information on the local electronic structure. We observe a $(5 \times \sqrt{3})$ stripe phase after annealing the phenoxy-terminated SAMs and obtain molecularly resolved images of the stripes. RAIRS, ellipsometry, and contact angle measurements provide complementary information needed to derive a molecular structure for the observed stripes. We believe that the initial SAM formation is driven by chain–chain van der Waals interactions, just like for normal long-chain alkanethiols, but that the formation of stripes with annealing is driven by phenoxy–phenoxy electrostatic interactions.

EXPERIMENTAL SECTION

Sample Preparation. One millimolar solutions of undecanethiol (C11) and 11-phenoxyundecanethiol (phenoxy) in ethanol were purchased from Asemblon Inc. and used without any further treatment. Au(111)/mica substrates were purchased from Agilent Technologies. These are gold films of at least 1500 Å epitaxially grown on cleaved mica. The substrates were cleaned by annealing with a hydrogen flame prior to use. Ethanol (200 proof, anhydrous) was purchased from Sigma-Aldrich and used as-is.

The monolayers were prepared by soaking the Au(111) substrates in the respective 1 mM solution for over 48 h at room temperature. The solutions were kept in the dark. After immersion, the samples were rinsed copiously with ethanol and dried under a stream of nitrogen gas to get rid of any physisorbed material. They were then transferred into the UHV chamber as quickly as possible.

Annealing of the monolayers was done in situ in our STM chamber (described below) using radiative heating from a tungsten filament mounted directly underneath the sample.

The temperature was monitored by a K-type thermocouple mounted on the sample surface for accurate measurement. The samples were usually left to cool back to room temperature overnight in UHV to minimize thermal drift during STM measurements.

STM/STS Measurements. STM measurements were made in a UHV 300 system (RHK Technology, Inc.) which houses a Besocke beetle, or “walker,” style STM. The base pressure of the chamber was less than 5×10^{-10} Torr. The STM tips were made either by mechanically cutting or chemically etching a PtIr wire (Pt80/Ir20, Goodfellow). Typical imaging parameters were 10 pA tunneling current and 0.5–1.5 V sample bias unless otherwise noted. All measurements were made at room temperature. STS measurements were made at preselected points within an STM image. As the imaging reaches the preselected points, the feedback loop is temporarily suspended while I – V curves are obtained. In this way, it is possible to know exactly where the STS measurements were taken.

RAIRS Measurements. RAIRS experiments were conducted in a UHV chamber described in detail elsewhere.²⁵ The samples were mounted on a five-axis manipulator. The RAIRS spectra were obtained using a Nicolet model 6700 infrared spectrometer (Fisher Thermo) with a liquid-nitrogen-cooled mercury cadmium telluride (MCT-A) detector. The infrared light was p-polarized and impinged on the sample at an incident angle of 75° . The spectra were collected at a resolution of 2 cm^{-1} and averaged over 500 scans.

Ellipsometry and Contact Angle Measurements. Ellipsometry measurements were made using a Gaertner L116S ellipsometer with a $\lambda = 633 \text{ nm}$ light source ($n_{\text{SAM}} = 1.5$, $n_{\text{Au}} = 0.2246 - 3.5i$). The results were averaged over values from five different spots on each sample.

Static water contact angle measurements were made by placing a microliter droplet of deionized water on the sample surface using a syringe infusion pump (Harvard Apparatus). The contact angles were measured on a two-dimensional projection of the droplet on the surface captured by a camera. Each reported angle is averaged over five measurements on the same substrate sample.

RESULTS

STM Measurements. STM images of a freshly prepared C11 SAM are shown in Figure 2. In the larger scale image

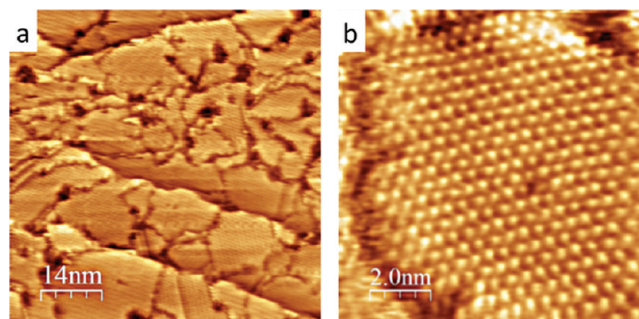


Figure 2. STM images of C11 SAM as-prepared in solution: (a) $70 \times 70 \text{ nm}^2$, 10 pA, 1.0 V, and (b) $10 \times 10 \text{ nm}^2$, 10 pA, 1.0 V. The $(\sqrt{3} \times \sqrt{3})R30^\circ$ structure is clearly observed in (b).

(Figure 2a), many etch pits and patches of close-packed standing phase separated by domain boundaries are seen, typical of solution-prepared alkanethiol SAMs.^{5,21} We observe

single gold-atom etch pits (2.5 \AA deep), resulting from significant reconstruction of the underlying Au(111) surface upon adsorption of the alkanethiol molecules.²⁶ A zoomed-in image (Figure 2b) reveals the well-known densely packed standing phase with the $(\sqrt{3}\times\sqrt{3})R30^\circ$ structure with respect to the underlying gold lattice.⁵

STM images of a freshly prepared phenoxy SAM are shown in Figure 3a. Lots of small pits (typically $<5 \text{ nm}$ across) are

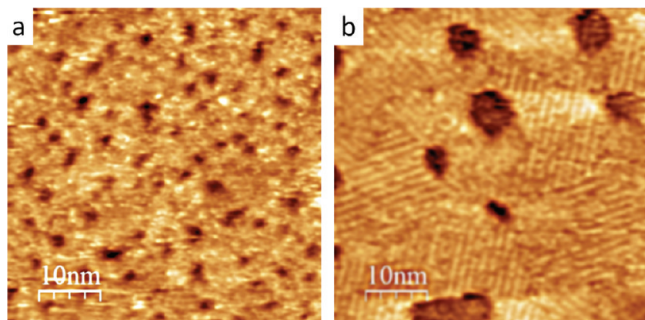


Figure 3. $50 \times 50 \text{ nm}^2$ STM images of (a) a freshly prepared phenoxy SAM, acquired at 1.3 V and 10 pA, and (b) an annealed phenoxy SAM, acquired at 1.4 V and 10 pA. Before annealing, the surface appears disordered and small etch pits are scattered about (a), but after annealing, domains of stripes appear, and the etch pits have coalesced into larger ones due to Ostwald ripening (b).

observed which appear to be about 2.3 \AA deep. These are most likely etch pits analogous to those on unsubstituted alkanethiol SAMs, indicating that the phenoxy molecules are chemisorbed onto the gold through the sulfur atom.²⁷ Other than these etch pits, the surface appears rather featureless and no molecular resolution was obtained, indicating that the surface is disordered and/or that the molecules are mobile or unstable with respect to imaging.

Since the phenoxy molecules may be kinetically trapped into a disordered state during the formation process, we heated the phenoxy SAM to try and find a more thermodynamically favored state with long-range order. Annealing was done in situ at 350–360 K for 2–4 h. This resulted in the formation of domains of stripes rotated 120° from each other as shown in Figure 3b, as well as fewer but larger etch pits due to Ostwald ripening.²⁸ The measured interstripe spacing is $14.4 \pm 0.4 \text{ \AA}$, and the corrugation is about 0.6 \AA . Since the backbone chain alone of the phenoxy molecule up to the O atom is about 15 \AA long, the molecules cannot be lying down flat on the substrate to form the stripes.

A zoomed-in image of the stripes is shown in Figure 4a. High-resolution images typically show that the stripes consist of a pair of rows where one appears to have clear dotlike features along the row while the other usually appears less resolved. As labeled in Figure 4a, we will be calling them row X and Y, respectively, for the purposes of this work. We can also see from the image that both rows consist of features along the stripe that are about 5 \AA apart. Since the Au(111) surface is a hexagonally close-packed structure with an atom-to-atom spacing of 2.88 \AA , 5 \AA corresponds to the next-nearest-neighbor distance of the Au atoms on the surface. This suggests that the stripes are running along the $\langle 121 \rangle$ direction of the Au(111) surface.²⁹ The features along one row X to another are not staggered but directly across from each other, and the spacing of 14.4 \AA matches the distance between five nearest-neighbor Au atoms, so the stripe phase has a $(5\times\sqrt{3})$

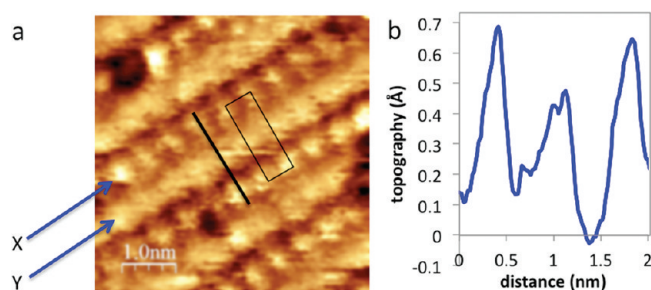


Figure 4. (a) A $5 \times 5 \text{ nm}^2$ STM image of the stripe phase of an annealed phenoxy SAM where molecular resolution is achieved, acquired at 0.7 V and 10 pA. Two rows of molecules are visible within each stripe—one has clear dotlike features (labeled X) and the other is less clearly resolved (labeled Y). The rectangle in the image indicates a unit cell of the $(5\times\sqrt{3})$ rectangular structure. (b) Line scan over the black line in the STM image showing the height corrugation.

rectangular structure, following the notation by Poirier and co-workers.³⁰ A unit cell is drawn over the image in Figure 4a where the short edges are defined by rows X. We can see that the features in row Y appear slightly staggered from the features in row X. While row Y is running roughly through the center of two X-rows, line scans of the image show that there is a sharp boundary between row Y and only one of the neighboring X-rows. Lee et al. have also observed a $(5\times\sqrt{3})$ rectangular structure for pyrrolyl-terminated long-chain alkanethiol SAMs, but they were not able to obtain molecular resolution images.²³

For structural comparison, the C11 SAM was annealed in situ at 380 K for 2 h. The resulting STM images of the annealed surface consisted of areas of the dense $(\sqrt{3}\times\sqrt{3})R30^\circ$ phase as well as a significant amount of stripe phase as seen in Figure 5a. Two different types of stripes were observed. The wider stripes have a spacing of $32.6 \pm 2.5 \text{ \AA}$ and a height corrugation of about 0.8 \AA (Figure 5b), and the narrower stripes have a spacing of $23.0 \pm 1.2 \text{ \AA}$ and height corrugation of about 0.6 \AA (Figure 5c). These stripe spacings match those reported by Ripsan et al. for an annealed C11 SAM, corresponding to $(11.5\times\sqrt{3})$ and $(8\times\sqrt{3})$ structures, respectively.³¹ These results are markedly different from those of the annealed phenoxy SAM, showing once again that the phenoxy terminal group greatly affects the structure of the SAM.

We made STS measurements over a large area of the phenoxy SAM stripes using RHK's data acquisition software. Some data sets turned out to be inconsistent, reflected by the tip changes that occurred frequently during imaging. However, there were indeed many sets of spectra that were consistent and exhibited distinct features. The averages of these sets of eight curves are shown in Figure 6 along with their corresponding dI/dV curves derived mathematically from the software. The $I-V$ curves in sets A and B have similar characteristics. They have an energy gap, and on the positive sample bias side, there is a quick rise in current around a certain bias (1.0 V for A, 0.5 V for B) followed by a much slower increase with increasing bias, resulting in a peak in the corresponding dI/dV curves. The tunneling current is typically proportional to the local density of states (LDOS), and peaks in the dI/dV curve indicate that there are discrete energy levels at the point of measurement.^{32,33} This suggests that the curves A and B were taken over phenoxy groups and we are accessing a molecular state of them, most likely the LUMO, when the current increases. The peak positions in the dI/dV curves differ by about 0.5 V for A and B, which may indicate that there are phenoxy species in

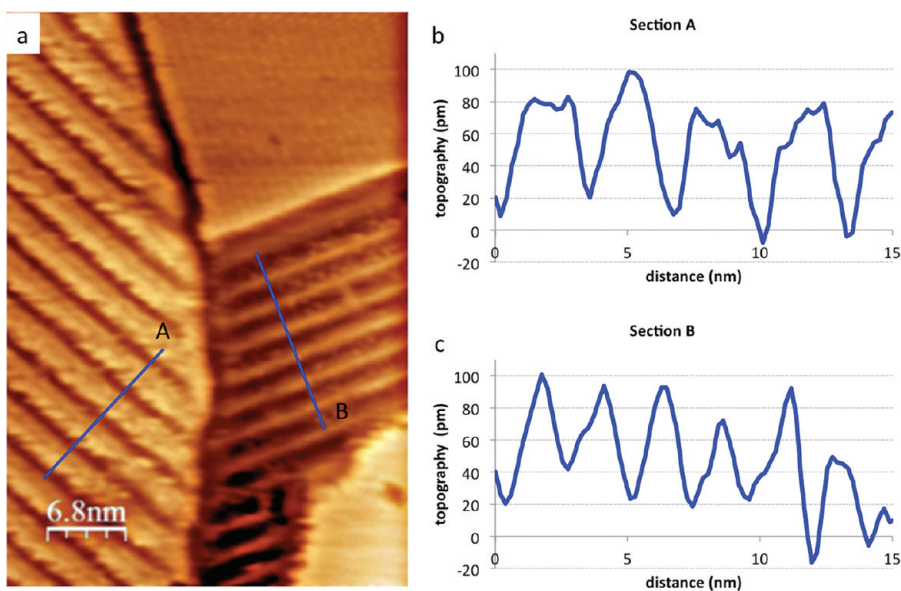


Figure 5. (a) A $36.3 \times 51.1 \text{ nm}^2$ STM image of a C11 SAM after annealing at 380 K for 2 h, acquired at 0.8 V and 10 pA. Areas with the densely packed ($\sqrt{3} \times \sqrt{3}$)R30° structure are seen in the top right and bottom right of the STM image. Two different stripe phases are also observed. (b) The spacing of the wider stripes is $32.6 \pm 2.5 \text{ \AA}$, measured from trough to trough, with a height corrugation of about 0.8 Å. (c) The spacing of the narrower stripes is $23.0 \pm 1.2 \text{ \AA}$, measured from peak to peak, with a height corrugation of about 0.6 Å. Measurements were taken along multiple lines parallel to those shown in (a). The y-axis for both line scans is offset by an arbitrary amount.

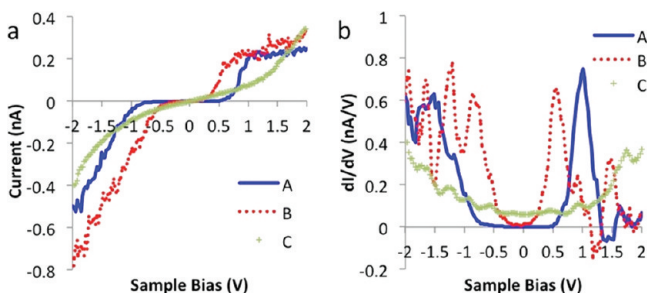


Figure 6. (a) STS spectra taken over large domains of stripes on an annealed phenoxy SAM. Each spectrum is an average of eight individual spectra taken over a same point on the sample. The imaging parameters before the feedback was cut off were 1.3 V and 10 pA. (b) Corresponding dI/dV curves, derived mathematically by the data acquisition software. It is clear that an energy gap exists for spectra A and B, but not for C.

two different environments on the surface. On the negative sample bias side, the $I-V$ curves for both A and B are noisy and appear to decrease exponentially after the energy gap. This could be caused by the tip, especially if there are molecules dangling from it, since the negative sample bias side is heavily affected by the tip's unoccupied electronic structure.^{34,35} We also observed $I-V$ curves with no energy gap exhibiting a relatively smooth curvature as represented in set C. These are similar to spectra taken on a normal alkanethiol SAM.^{36,37} This suggests that some parts of the backbone alkyl chains may be exposed to the surface.

We performed bias-dependent imaging as well and observed that sometimes there were repeatable, noticeable changes in the image as the bias was varied. We attempt to explain these changes using our STS results. In Figure 7, we see alternating rows of ellipses and blurry lines at a sample bias of 1.0 V. The rows of ellipses most likely correspond to rows X that we observed earlier, and the blurry lines to rows Y. The elliptical features suggest that the plane of the phenyl rings is close to or

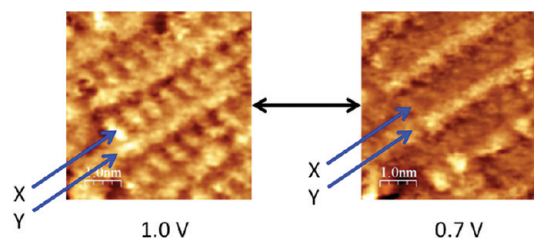


Figure 7. Bias-dependent STM imaging of the phenoxy stripes acquired at 10 pA of a $5 \times 5 \text{ nm}^2$ area. Elliptical features of rows X visible at 1.0 V seem to disappear at 0.7 V.

exactly perpendicular to the surface. When the bias is lowered to 0.7 V, the rows X seem to disappear. This could be explained by looking at $I-V$ curves A and B in Figure 6. At 1.0 V, the current signal is about the same for both, but when the bias is decreased to 0.7 V, the signal for A drops significantly, whereas the signal for B only decreases slightly. If A corresponds to the ellipses in row X, and B to the molecules forming row Y, this would result in the elliptical features being heavily suppressed in the 0.7 V image, which is what we observe.

RAIRS Measurements. The spectra from the RAIRS measurements are shown in Figure 8, and the peak assignments are shown in Table 1 along with data of the transmission IR spectrum of the neat phenoxy molecules taken previously by Cavadas.¹⁹ Cavadas and Anderson have also previously taken RAIRS measurements on an unannealed phenoxy SAM, and our results for a freshly prepared phenoxy SAM largely match theirs.³⁸ (Our freshly prepared phenoxy SAMs appear to be a little more well ordered than theirs, perhaps due to our longer soak time in solution.) The peak position and fwhm of the asymmetric CH_2 vibrational mode of the backbone alkyl chain are sensitive to the degree of chain-chain interactions and how well-ordered the SAM is.^{18,39} The values obtained for the phenoxy SAMs are shown in Table 2, along with the values for a well-ordered standing-phase undecanethiol SAM (before

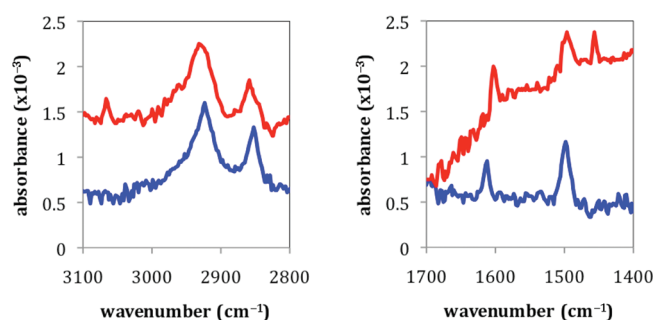


Figure 8. RAIRS spectra of the phenoxy SAMs. The blue line represents the freshly prepared SAM, and the red line represents the SAM after annealing. The absorbance values were offset for clarity.

Table 1. Peak Locations and Assignments of the Transmission IR Spectra of the Neat Phenoxy Molecules,¹⁹ and of the RAIRS Spectra of the Phenoxy SAMs before and after Annealing, Compared to Literature RAIRS Values of the As-Prepared Phenoxy SAMs

transmission IR (cm ⁻¹) ¹⁹	RAIRS (cm ⁻¹)			assignment ⁴¹
	as-prepared, this expt	as-prepared, lit. ¹⁹	after annealing	
3066	—	—	3067	phenyl CH str
2915	2923	2925	2930	—CH ₂ — asym str
2846	2852	2852	2859	—CH ₂ — sym str
1596	1611	1608	1603	C—C ring str
1500	1498	1496	1496	C—C ring str
1486	—	—	1456	C—C ring str
1245	—	—	—	C—O str

Table 2. RAIRS Peak Positions of the CH₂ Stretching Modes and Fwhm of the CH₂ Asymmetric Stretching Mode Peak of the Phenoxy SAMs before and after Annealing, Compared to the Values for an Undecanethiol SAM before and after Annealing

SAM	CH ₂ , asym str position (cm ⁻¹)	CH ₂ , asym str fwhm (cm ⁻¹)	CH ₂ , sym str position (cm ⁻¹)
1-undecanethiol, as-prepared	2921	9	2851
1-undecanethiol, stripe phase	2908	11	—
phenoxy, as-prepared	2923	17	2852
phenoxy, after annealing	2930	26	2859

annealing) and a lying-down-phase one (after annealing) for comparison. Our results for the undecanethiol SAMs closely match those from previous literature for decanethiol SAMs which behave similarly.⁴⁰ For the freshly prepared phenoxy SAM, the asymmetric CH₂ peak appears at 2923 cm⁻¹ with a fwhm of 17 cm⁻¹. The peak position only shifted to a slightly higher wavenumber and the fwhm increased by 8 cm⁻¹ compared to a well-ordered dense undecanethiol SAM, indicating some increase in disorder of the alkyl chain portion of the phenoxy SAM, but the chains are largely unaffected by the phenoxy terminal group. This drastically changes once the phenoxy SAM is annealed—the peak position shifts further up to 2930 cm⁻¹ and the fwhm increases to 26 cm⁻¹. Annealing has resulted in reduced chain–chain interactions and/or more disorder of the phenoxy SAM. No peak is observed around

2908 cm⁻¹, so the chains are not lying down on the substrate. Also, the peak intensities did not decrease significantly, so not much desorption took place during annealing. In sum, the as-prepared phenoxy SAM is in a dense phase and makes a dramatic transition to an intermediate phase as it is annealed.

The peaks related to the phenyl rings provide information about the orientation of the rings with respect to the surface and to each other. Before annealing, only two peaks of the phenyl ring modes appear—one at 1611 cm⁻¹ and the other at 1498 cm⁻¹. These are both assigned to ring stretching modes along the molecular axis running through the ring C—O bond in the plane of the ring.⁴¹ After annealing, these two peaks are still present at 1603 and 1496 cm⁻¹, but two additional peaks appear at 1456 and 3067 cm⁻¹. The peak at 1456 cm⁻¹ is assigned to the in-plane ring stretching mode perpendicular to the molecular axis running through the ring C—O bond.⁴¹ The peak at 3067 cm⁻¹ is assigned to an aromatic C—H stretching mode involved in edge-to-face interactions of the phenyl rings.¹⁹ The above data indicate that before annealing, the phenyl rings are in a standing-up position relative to the substrate surface with the molecular axis running through the ring C—O bond perpendicular or near-perpendicular to the surface, and that edge-to-face interactions of the rings are prohibited. After annealing, the phenyl rings are canted so that all of the ring stretching modes have components perpendicular to the surface, and there are edge-to-face interactions of the rings.

Ellipsometry and Contact Angle Measurements. Ellipsometry measurements were made on the phenoxy SAMs to determine the film thickness. The thickness of the freshly prepared phenoxy SAM was measured to be 19.2 ± 2.0 Å, which is in agreement with previous literature.³⁸ This value corresponds well to the case where the backbone alkyl chain of the phenoxy molecule is tilted about 30° from the surface normal, just as in a normal alkanethiol SAM to maximize the chain–chain van der Waals interactions, and the molecule twisted so that the phenyl ring is perpendicular to the surface. After annealing the phenoxy SAM, ellipsometry showed that the film thickness decreased significantly to 10.8 ± 3.9 Å. This suggests that the phenoxy molecules are tilted farther away from the surface normal after annealing.

Water contact angle measurements were made on the phenoxy SAMs to obtain qualitative information on the exposure of the polar ether linkage to the film surface. The contact angle on a freshly prepared phenoxy SAM was 93 ± 2°, indicating the SAM is hydrophobic and the ether linkage is buried within the film. After annealing, the value decreased slightly to 78 ± 4°, indicating increased ether linkage exposure at the film surface after annealing.

DISCUSSION

STM/STS, RAIRS, ellipsometry, and contact angle measurements all provide separate fragments of information on how the structure of the phenoxy SAM changes before and after annealing. STM gave us local images of the film surface, and the other three techniques provided information related to the orientation of the molecules averaged over the entire sample. With all the fragments combined, we can gain a good understanding of the structural changes that occur in the phenoxy SAM.

For the freshly prepared phenoxy SAM, the film surface looked disordered with the STM, while according to RAIRS, the crystallinity of the alkyl chains is not very different from that of a normal well-ordered alkanethiol SAM. This indicates

that the disorder is largely localized to the film surface near the phenoxy end group. In addition, RAIRS showed that all of the phenyl rings are oriented near-perpendicular to the surface. Ellipsometry and water contact angle measurements agree with the above picture as well. A previous NEXAFS study of phenoxy SAMs by Luk et al. also showed that the phenyl rings are on average close to being perpendicular to the surface, and that the backbone alkyl chains have a similar tilt angle to a normal alkanethiol SAM.⁴² Luk et al. also observed in the same study that the angular dependence of the π_1^* resonance of the phenyl rings is not very strong, indicating that the rings are only partially ordered. Since STM can only look at the very surface of the film (without disrupting the film using high tunneling currents), we can conclude that the freshly prepared phenoxy SAM is in a high-density phase with the backbone alkyl chain layer largely similar to that of a normal standing-phase alkanethiol SAM. However, the ordering of the chains does not lead to a crystalline packing of the terminal phenoxy group, even though it forces the phenyl rings to stand perpendicular to the surface.

The fact that the as-prepared phenoxy SAM is not entirely crystalline is somewhat expected considering the slightly bulky phenoxy terminal group and how it can affect the formation of the monolayer in solution. In general, after initial rapid adsorption of the thiols onto the gold substrate, the monolayer goes through a slow consolidation process, and the kinetics of this process is affected by chain disorder and molecular interactions.^{2,4} According to Laibinis and co-workers, an ether moiety possesses a significant permanent dipole that makes gauche conformations of the chain slightly favorable, especially if the ether linkage is at the end of the alkane chain.⁴³ For long alkane chains with greater than nine carbons, the van der Waals attraction energy should dominate the molecular interactions,⁴ but the polar–polar interaction between the phenoxy groups may compete against it, as well as phenyl–phenyl interactions. Also, the van der Waals diameter of the alkane chain is 4.5 Å, whereas that of the phenyl group is 6.3 Å.⁴⁴ This may hinder the formation of the densely packed ($\sqrt{3}\times\sqrt{3}$)R30° phase where the nearest-neighbor spacing is 5 Å, although it has been shown previously that phenyl-terminated SAMs with no ether linkage form well-ordered structures analogous to normal alkanethiol SAMs, where the phenyl rings interact in an edge-to-face configuration.^{18,21,38}

From our RAIRS results, we see that the chain–chain van der Waals interaction does indeed dominate the initial monolayer formation, causing the chains to stand up and form a close-packed structure. The phenoxy group is not bulky enough to mask adsorption sites. However, the film is not as ordered as it could be compared to a normal dense alkanethiol SAM—the peak position of the asymmetric CH₂ vibrational mode shifted higher by 2 cm⁻¹, and its fwhm increased by 8 cm⁻¹ (Table 2). The disruption must originate from the highly polar ether linkage since analogous phenyl-terminated SAMs form well-ordered structures.³⁸ Normally, the edge-to-face interaction between two phenyl rings is between a partially positively charged hydrogen and a partially negatively charged ring.⁴⁵ However, an alkoxy substituent on the ring has an electron-withdrawing inductive effect and an electron-donating resonance effect.⁴⁶ These effects can affect the electrostatic and London dispersion interactions which stabilize the edge-to-face interaction of the phenyl rings.⁴⁷ Since edge-to-face interactions exist in the phenoxy molecule's neat form according to its transmission IR spectra,¹⁹ the interaction must still be favorable,

but it is probably highly orientation-specific. During the monolayer formation in solution, the chain–chain interactions dominate and the phenoxy–phenoxy interactions only manage to cause a small disturbance to the close-packing of the chains. With limited mobility due to the close-packed chains, the phenoxy groups likely cannot pack into any favorable configuration and remain disordered. Even if the phenoxy groups are roughly ordered simply from the close-packing of the chains, if they are not pinned into a stable configuration, the STM tip can perturb the phenoxy groups as it scans over them, making the surface appear disordered under the microscope.

When the phenoxy SAMs are annealed at above 350 K for 2 h or more, their structure changes significantly according to all of the techniques we used. First of all, we see stripes with the STM with an interstripe spacing of 14.4 Å and features within the stripes that are 5 Å apart. The stripes appear to consist of at least two different parts (rows X and Y), but we need to bring in information from the other techniques to determine the detailed structure of the stripes. Ellipsometry shows us that the film thickness almost halved from 19.2 ± 2.0 Å before annealing to 10.8 ± 3.9 Å after annealing. Since ellipsometry is an averaging technique, it is possible that half of the molecules are standing up and half lying down, but the measured stripe spacing is too small for the molecule to be lying down, and we would expect the film to be much more hydrophilic from the high exposure of the ether linkage. Also, the measured corrugation of the stripes was rather small (about 0.6 Å). Barrena et al. have previously observed a stable ($4\times\sqrt{3}$) rectangular decanethiol SAM structure with a $\sim 50^\circ$ tilt angle of the chains with respect to the surface normal, stabilized by the van der Waals interaction with the gold substrate.⁴⁸ If the phenoxy molecule were at a 50° tilt angle, the vertical height from the sulfur to the oxygen will be about 10.3 Å which is close to the ellipsometry measurement. The annealed phenoxy SAM may well be based on this 50° tilt structure.

We now turn to RAIRS for the last pieces of the puzzle. Regarding the backbone alkyl chain after annealing, the peak position of the asymmetric CH₂ vibrational mode of the phenoxy SAM shifted higher by 9 cm⁻¹, and its fwhm increased by 17 cm⁻¹ relative to a normal dense alkanethiol SAM (Table 2). These are significant changes indicating reduced chain–chain interactions. The absence of a peak around 2908 cm⁻¹ indicates the chains are not lying down on the substrate. If we assume that the phenoxy molecules are tilted by 50° , the chains have to be spaced out more than if they were tilted by 30° , so there will indeed be less chain–chain interactions. There are also important changes we see in the peaks related to the phenyl ring after annealing. The presence of all of the ring stretching modes indicate that the rings are canted, and the appearance of the peak for the aromatic C–H stretching mode suggests that the phenyl rings are in an edge-to-face configuration. The edge-to-face configuration implies that there are phenyl rings in two different orientations which are likely the origins of rows X and Y in our high-resolution STM images. Combining our observed ($5\times\sqrt{3}$) rectangular structure with double rows and our hypothesis that the molecules are tilted by 50° , we see that it is impossible to find a plausible structure of the phenoxy stripes if we assume that all of the phenoxy molecules are in the all-trans state. The backbone chain up to the ether linkage casts a 11.6 Å shadow at a 50° tilt angle, and the row-to-row spacing in the double rows would be 4.3 Å if they were close-packed, so the phenyl rings will have to stand perpendicular to the surface in order to

obtain edge-to-face ring interactions. However, our RAIRS results do not support this configuration, and we have established from the results of the unannealed SAM that the edge-to-face configuration in an all-perpendicular state is not favored. Since ellipsometry is an averaging technique, it is possible that the chain tilt angles are varied, but the resulting significant decrease in chain–chain interactions makes it highly unlikely. Therefore, we propose that gauche conformations exist in the alkyl chains. As was mentioned earlier, an ether linkage can cause gauche conformations. According to Laibinis et al., the dipole moment exerts an electrostatic effect on the chain ordering, and the gauche conformation is generally favored over an all-trans configuration by 0.1–0.2 kcal/mol.⁴³ With the introduction of gauche conformations, we can arrange the phenoxy molecules so that the rings are in an edge-to-face configuration where some of the rings are canted, thereby satisfying all of the data that we have obtained.

Our proposed structure of the annealed striped phenoxy SAM is shown in Figure 9. The structure is based on the

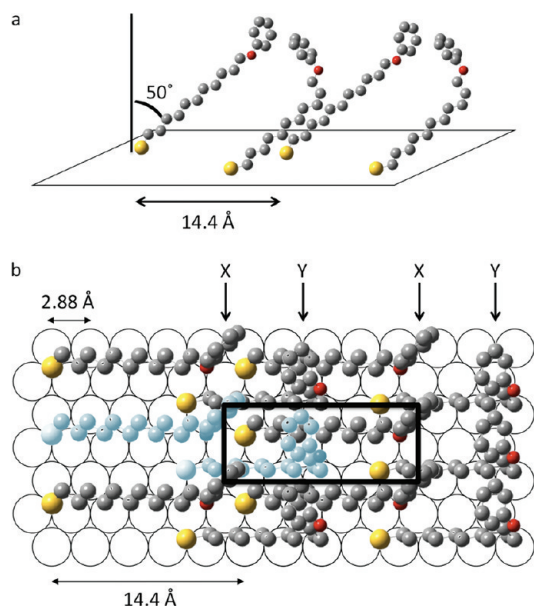


Figure 9. Schematics of our proposed structure of the phenoxy stripes. (a) Side view showing two pairs of molecules with interacting phenyl rings. The molecules are tilted 50° from the surface normal. (b) Top view: A pair of molecules with interacting phenyl rings are highlighted in blue, and the rows of phenyl rings corresponding to rows X and Y are labeled. The rectangle denotes the unit cell of the stripe structure. The circles represent gold atoms of the substrate surface. The 3-fold site was picked as the adsorption site for schematic purposes.

$(5\sqrt{3})$ rectangular structure that we see with the STM with each stripe consisting of two parts. Within each stripe, the sulfur atoms are placed in next-nearest-neighbor positions so that the chains can interact as much as possible. This is also consistent with our high-resolution STM images where we see features within the stripes that are 5 Å apart, suggesting that the stripes are running along the $\langle 121 \rangle$ direction of the Au substrate.²⁹ The chain tilt angle is 50° based on the film thickness measured by ellipsometry and on a stable $(4\sqrt{3})$ rectangular decanethiol SAM structure reported by Barrena et al.⁴⁸ On the basis of the information from RAIRS, we propose that one part of the stripes is made up of phenoxy molecules that have a gauche conformation near the ester

linkage so that they can interact favorably in an edge-to-face configuration with the other part of the stripe. Since the features in rows X sometimes appeared elliptical, we believe the phenyl rings in them are perpendicular or near-perpendicular to the surface. In our proposed stripe structure, rows X would correspond to the lines formed by the phenyl rings on the all-trans molecules, and rows Y to those formed by the rings on the kinked molecules. This structure is also consistent with our water contact angle measurements—the surface of the annealed film still primarily consists of hydrophobic phenyl rings, but the structure is more open compared to the unannealed phenoxy SAM so the hydrophilic ether linkage is less shielded than before.

We believe that the transition of the phenoxy SAM in its packed state to the stripe phase with annealing is driven mainly by the terminal phenoxy groups. From our results of the freshly prepared phenoxy SAM, we saw that the chain–chain interactions dominate the SAM formation in solution, and that the phenoxy terminal groups do not end up in a favorable configuration. According to Yang and Liu, the two-dimensional melting temperature of a decanethiol SAM is about 345 K and that of a dodecanethiol SAM is about 367 K,²¹ so our annealing temperature of 350–360 K should be right around the two-dimensional melting temperature of our phenoxy molecules that have 11 carbons. During the melting process the chains become more mobile and can go through conformational changes, and some desorption starts to happen above the melting temperature, although significant desorption should only occur above 400 K.^{20,21,49} In the case of the as-prepared phenoxy SAM, the molecules may be destabilized by adverse interactions between the phenoxy groups and desorption may occur more easily. With the chains being mobile and some desorption taking place during annealing, some of the molecules will have more room to rotate around into the gauche conformation, which should be favored energetically by about 0.1–0.2 kcal/mol as mentioned earlier.⁴³ Also, to compensate for some of the lost chain–chain interaction, the chains may start to tilt more for better van der Waals interaction with the gold substrate. During these processes, the phenyl rings find a favorable edge-to-face configuration, and as the SAM cools down after the anneal, the configuration persists. Barrena et al. have calculated from a simple model that alkanethiols with nine carbons or less will prefer the 50° tilt structure.⁴⁸ Due to the presence of the polar ether linkage and the gauche conformation induced by it, the closest neighboring chain–chain interaction stops after about nine carbons. The chain–chain attractive energy is on the order of 1.4–1.8 kcal/mol per CH_2 ,³ and the face-to-edge interaction for a benzene dimer is about 2.2–2.4 kcal/mol.⁴⁷ In our proposed stripe structure, the loss of a couple of units of chain–chain interactions between neighboring molecules can be partially compensated by the face-to-edge interaction, and the loss of two closest neighboring chains could be partially compensated by the larger van der Waals interaction with the gold substrate due to greater tilt. Also, we believe unfavorable interactions of the phenoxy groups that may decrease the stabilization energy of the monolayer are avoided.

CONCLUSIONS

Solution-deposited phenoxy SAMs on Au(111)/mica substrates were studied with UHV STM/STS, RAIRS, ellipsometry, and water contact angle measurements. We observed that the chain–chain van der Waals interactions dominate the formation

of the as-prepared SAM to form a close-packed film, analogous to normal long-chain alkanethiols, with relatively minor disruptions due to the phenoxy terminal group. However, the phenoxy groups are locally disordered and not well-packed in this configuration, and the film looks disordered under the STM. When the phenoxy SAM is annealed at 350–360 K in vacuum, domains of stripes are formed. The stripes have a $(5\sqrt{3})$ rectangular structure with respect to the Au(111) substrate, running along the $\langle 121 \rangle$ crystallographic direction. We find a clear structural solution to the stripe configuration that satisfies the results from all four techniques we used. The stripe phase is a slightly lower density phase where each stripe is made from two rows of molecules: one row consists of molecules with a gauche conformation and the second row is composed of all-trans molecules so that the phenyl rings from each of the rows can interact in a favorable edge-to-face configuration. We believe that the chains within each stripe are close-packed to maximize the chain–chain van der Waals interaction. The molecules are tilted 50° from the surface normal for better van der Waals interaction with the gold substrate to compensate for some of the decreased chain–chain interactions due to the overall lower coverage. Whereas the initial SAM formation is driven by chain–chain interactions, we believe the transition to the stripe phase is driven mainly by phenoxy–phenoxy interactions.

These characteristics of the phenoxy SAMs are different from phenyl-terminated SAMs where the film is crystalline in the as-prepared state,¹⁸ and also from pyrrolyl-terminated SAMs where the STM results looked very similar but the results from their other techniques led to a different stripe structure.²³ The importance of using multiple techniques to investigate SAM structures cannot be overemphasized. The fact that the phenoxy SAMs behaved somewhat similarly to pyrrolyl-terminated SAMs than to phenyl-terminated SAMs suggests that polar interactions or electrostatic effects are what cause disorder at the surface of the film, but what promote a striped structure when the SAMs are annealed.

AUTHOR INFORMATION

Corresponding Author

*Email: s-sibener@uchicago.edu.

Notes

The authors declare no competing financial interest.

ACKNOWLEDGMENTS

This work was funded by the Office of Basic Energy Sciences, Office of Science, U.S. Department of Energy, Grant DE-SC0002583, and infrastructure support from the NSF-Materials Research Science and Engineering Center at The University of Chicago. Seed funding for this work was provided by DTRA Grant No. HDTRA1-11-1-0001. The authors thank Gaby Avila-Bront for assistance in image processing.

REFERENCES

- (1) Nuzzo, R.; Allara, D. *J. Am. Chem. Soc.* **1983**, *105*, 4481.
- (2) Bain, C.; Troughton, E.; Tao, Y.; Evall, J.; Whitesides, G.; Nuzzo, R. *J. Am. Chem. Soc.* **1989**, *111*, 321.
- (3) Dubois, L. H.; Nuzzo, R. *Annu. Rev. Phys. Chem.* **1992**, *43*, 437.
- (4) Ulman, A. *Chem. Rev.* **1996**, *96*, 1533.
- (5) Poirier, G. *Chem. Rev.* **1997**, *97*, 1117.
- (6) Schreiber, F. *Prog. Surf. Sci.* **2000**, *65*, 151.
- (7) Chidsey, C. E. D.; Loiacono, D. N. *Langmuir* **1990**, *6*, 682.

- (8) Widrig, C. A.; Alves, C. A.; Porter, M. D. *J. Am. Chem. Soc.* **1991**, *113*, 2805.
- (9) Nuzzo, R. G.; Dubois, L. H.; Allara, D. L. *J. Am. Chem. Soc.* **1990**, *112*, 558.
- (10) Fenter, P.; Eberhardt, A.; Liang, K. S.; Eisenberger, P. *J. Chem. Phys.* **1997**, *106*, 1600.
- (11) Whitesides, G.; Laibinis, P. *Langmuir* **1990**, *6*, 87.
- (12) Bain, C. D.; Whitesides, G. M. *Angew. Chem., Int. Ed.* **1989**, *28*, 506.
- (13) Chidsey, C. E. D. *Science* **1991**, *251*, 919.
- (14) Jin, Q.; Rodriguez, J. A.; Li, C. Z.; Darici, Y.; Tao, N. *J. Surf. Sci.* **1999**, *425*, 101.
- (15) Chen, W.; Huang, C.; Gao, X. Y.; Wang, L.; Zhen, C. G.; Qi, D.; Chen, S.; Zhang, H.; Loh, K. P.; Chen, Z. K.; Wee, A. T. S. *J. Phys. Chem. B* **2006**, *110*, 26075.
- (16) Tao, Y.; Wu, C.; Eu, J.; Lin, W. *Langmuir* **1997**, *13*, 4018.
- (17) Jung, H. H.; Won, Y. D.; Shin, S.; Kim, K. *Langmuir* **1999**, *15*, 1147.
- (18) Lee, S.; Puck, A.; Graupe, M.; Colorado, R.; Shon, Y.; Lee, T.; Perry, S. *Langmuir* **2001**, *17*, 7364.
- (19) Cavadas, F. T. *Spectroscopic and Electrochemical Investigation of Phenyl, Phenoxy, and Hydroxyphenyl-Terminated Alkanethiol Monolayers*; Virginia Polytechnic Institute and State University: Blacksburg, VA, 2003.
- (20) Qian, Y.; Yang, G.; Yu, J.; Jung, T.; Liu, G. *Langmuir* **2003**, *19*, 6056.
- (21) Yang, G.; Liu, G. *J. Phys. Chem. B* **2003**, *107*, 8746.
- (22) Duan, L.; Garrett, S. *Langmuir* **2001**, *17*, 2986.
- (23) Lee, J. S.; Chi, Y. S.; Kim, J.; Yun, W. S.; Choi, I. S. *J. Phys. Chem. Chem. Phys.* **2008**, *10*, 3138.
- (24) Sethuraman, A.; Han, M.; Kane, R. S.; Belfort, G. *Langmuir* **2004**, *20*, 7779.
- (25) Yuan, H.; Killelea, D. R.; Tepavcevic, S.; Kelber, S. I.; Sibener, S. J. *J. Phys. Chem. A* **2011**, *115*, 3736.
- (26) Vericat, C.; Vela, M. E.; Benitez, G.; Carro, P.; Salvarezza, R. C. *Chem. Soc. Rev.* **2010**, *39*, 1805.
- (27) Poirier, G. *Langmuir* **1997**, *13*, 2019.
- (28) Cavalleri, O.; Hirstein, A.; Kern, K. *Surf. Sci.* **1995**, *340*, L960.
- (29) Poirier, G. *Langmuir* **1999**, *15*, 1167.
- (30) Poirier, G.; Tarlov, M.; Rushmeier, H. *Langmuir* **1994**, *10*, 3383.
- (31) Ripsan, A.; Li, Y.; Tan, Y. H.; Galli, G.; Liu, G.-y. *J. Phys. Chem. A* **2007**, *111*, 12727.
- (32) Tersoff, J.; Hamann, D. R. *Phys. Rev. B* **1985**, *31*, 805.
- (33) Datta, S.; Tian, W.; Hong, S.; Reifenberger, R.; Henderson, J. I.; Kubiak, C. P. *Phys. Rev. Lett.* **1997**, *79*, 2530.
- (34) Klitsner, T.; Becker, R. S.; Vickers, J. S. *Phys. Rev. B* **1990**, *41*, 3837.
- (35) Torrente, I. F.; Franke, K. J.; Pascual, J. I. *J. Phys.: Condens. Matter* **2008**, *20*, 184001.
- (36) Kobayashi, K.; Horiuchi, T.; Yamada, H.; Matsushige, K. *Thin Solid Films* **1998**, *331*, 210.
- (37) Pflaum, J.; Bracco, G.; Schreiber, F.; Colorado, R.; Shmakova, O.; Lee, T.; Scoles, G.; Kahn, A. *Surf. Sci.* **2002**, *498*, 89.
- (38) Cavadas, F. T.; Anderson, M. R. *J. Colloid Interface Sci.* **2004**, *274*, 365.
- (39) Nuzzo, R.; Fusco, F. A.; Allara, D. *J. Am. Chem. Soc.* **1987**, *109*, 2358.
- (40) Picraux, L. B.; Zangmeister, C. D.; Batteas, J. D. *Langmuir* **2006**, *22*, 174.
- (41) Varsanyi, G. *Vibrational Spectra of Benzene Derivatives*; Academic Press: New York, 1969.
- (42) Luk, Y. Y.; Abbott, N. L.; Crain, J. N.; Himpsel, F. J. *J. Chem. Phys.* **2004**, *120*, 10792.
- (43) Laibinis, P.; Bain, C.; Nuzzo, R.; Whitesides, G. *J. Phys. Chem.* **1995**, *99*, 7663.
- (44) Chang, S.; Chao, L.; Tao, Y. *J. Am. Chem. Soc.* **1994**, *116*, 6792.
- (45) Muehldorf, A. V.; Engen, D. V.; Warner, J. C.; Hamilton, A. D. *J. Am. Chem. Soc.* **1988**, *110*, 6561.

(46) Ege, S. *Organic Chemistry: Structure and Reactivity*, 4th ed.; Houghton Mifflin Co.: Boston, 1999.

(47) Jennings, W. B.; Farrell, B. M.; Malone, J. F. *Acc. Chem. Res.* **2001**, *34*, 885.

(48) Barrena, E.; Palacios-Lidon, E.; Munuera, C.; Torrelles, X.; Ferrer, S.; Jonas, U.; Salmeron, M.; Ocal, C. *J. Am. Chem. Soc.* **2004**, *126*, 385.

(49) Guo, Q.; Sun, X.; Palmer, R. *Phys. Rev. B* **2005**, *71*, 035406.